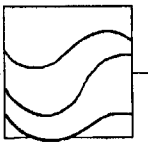

On altimetric data assimilation experiments in a linear model of the tropical Atlantic Ocean

Altimetry
Geosat
Numerical linear model
Dynamic height
Tropical Atlantic

Altimétrie
Geosat
Modèle numérique linéaire
Hauteur dynamique
Atlantique tropical

Bernard BOURLES [a], **Sabine ARNAULT** [b], **Christine PROVOST** [c]

[a] Centre ORSTOM de Cayenne, Guyane Francaise.

[b] Laboratoire d'Océanographie Dynamique et de Climatologie, Institut Français de Recherche pour le Développement en Coopération (ORSTOM), Université Paris VI, Paris, France.

[c] Laboratoire d'Océanographie Dynamique et de Climatologie, Centre National de la Recherche Scientifique, Université Paris VI, Paris, France.

ABSTRACT

We present results of sequential data assimilation of altimetric data in a linear tropical Atlantic model, using an analysis technique that we have developed. We use sea level anomaly fields obtained from altimetric data of the satellite Geosat. Despite the weak amplitudes of the anomaly fields, we obtain marked improvements of the model simulations due to assimilations. Thus, we show that altimetric data may be very useful for improving model simulations when adapted assimilation techniques are applied.

Oceanologica Acta, 1992. **15**, 5, 525-536.

RÉSUMÉ

Sur des expériences d'assimilation de données altimétriques dans un modèle linéaire de l'Océan Atlantique tropical

Nous présentons des résultats d'expériences d'assimilation séquentielle de données altimétriques dans un modèle linéaire de l'Océan Atlantique tropical. Nous assimilons des champs d'anomalies du niveau de la mer issus des mesures altimétriques du satellite Geosat. En dépit des faibles amplitudes des anomalies, nous observons des améliorations très nettes des simulations du modèle grâce aux assimilations. Nous montrons de ce fait que les données altimétriques peuvent se révéler très utiles pour améliorer les simulations des modèles en utilisant des techniques d'assimilation adaptées.

Oceanologica Acta, 1992. **15**, 5, 525-536.

INTRODUCTION

In contrast with *in situ* data, altimetric data can give global and quasi synoptic fields of the whole oceanic surface state. Recent studies have shown that satellite altimetry is a very helpful in the investigation of surface circulation in the tropical oceans (Miller *et al.*, 1986; Ménard, 1988; Miller and Cheney, 1990), which play a very important role in climatic variability, as the "El-Niño-Southern Oscillation" (ENSO) events show.

Due to the baroclinic character of the tropical oceans, sea level anomalies can be compared to dynamic height anomalies. Recent studies in the tropical Atlantic Ocean have demonstrated very good agreement between the seasonal

variability of the dynamic topography observed from *in situ* data and sea level obtained from altimetric data (Ménard, 1988; Arnault *et al.*, 1989; 1990).

During recent years, progress in modelling in the tropical oceans (Philander and Pacanowski, 1984; 1986; Morlière *et al.*, 1989) and investigation of data assimilation in tropical regions (Moore *et al.*, 1987; Leetma and Ji, 1989; Morlière *et al.*, 1989) have allowed us to consider an operational hindcasting of the tropical oceans state, by combining models and spatial and *in situ* observations using data assimilation methods, which is one of the objectives of the TOGA (Tropical Ocean Global Atmosphere) programme.

We have chosen to study the assimilation of altimetric data obtained from satellite measurements in a simple model of the tropical Atlantic Ocean. The linear model used and the altimetric data are presented first, before describing the assimilation technique developed for this study in the third section. In the fourth, we give a description and discussion of the results of the assimilation experiments, before concluding.

THE MODEL AND ALTIMETRIC DATA

The model

The tropical oceans can be characterized by a two-layer structure (an homogeneous and stable warm layer overlying a cold sub-thermoclinal layer). On large scales, we may describe the response of the tropical oceans by the thermocline depth (or dynamic height) variations which characterize fairly well the thermal and dynamic state of these oceans. Furthermore, we may compute mean geostrophic currents and estimate heat content variability over the sub-thermoclinal layer (Delcroix and Gautier, 1987) from dynamic height fields. The altimetric data we wish to assimilate give information on the sea-level anomaly that could be compared with the dynamic height anomaly, due to the baroclinic character of the tropical Atlantic Ocean.

Thus, we need a model which reliably reproduces dynamic height variations, and which is numerically cheap so that many experiments can be performed. Different studies have shown the ability of linear vertical mode models to reproduce the seasonal variability of the dynamic height (du Penhoat and Treguier, 1985). The model we use computes the linear response of the tropical Atlantic Ocean to the wind forcing through three baroclinic modes. Previous studies have shown that the first three baroclinic modes provide 95 % of the signal obtained with nine modes (du Penhoat and Tréguier, 1985) and allow to permit reproduction of the inter-annual variability of the dynamic height topography (du Penhoat and Gouriou, 1987).

The model domain is that of the tropical Atlantic Ocean and extends from 20°S to 20°N in latitude and from 60°W to 13°E in longitude. The grid spacing (Arakawa type C) is variable and depends on the areas of interest (in longitude, the resolution is 67 km near the African coast, 80 km near the American coast and 111 km at the centre of the basin; in latitude, it increases from 88 km at the equator to 139 km at the northern and southern boundaries) in order to resolve adequately the equatorial radius of deformation. The model equations are obtained from a linearization of the Navier-Stokes equations using the following classical approximations: hydrostaticity, incompressibility and adiabaticity. The linearization is made about a mean density profile, characteristic of the middle of the equatorial Atlantic Ocean (24°W).

Assuming that horizontal and vertical motions are separable, the pressure and the horizontal components of the velocity fields can then be written as:

$$u = \Sigma_n u_n (x, y, t).F_n (z) \quad (1)$$

$$v = \Sigma_n v_n (x, y, t).F_n (z) \quad (2)$$

$$p = \Sigma_n p_n (x, y, t).F_n (z) \quad (3)$$

where u_n, v_n and p_n are the horizontal components of the velocity and pressure fields respectively relative to each mode.

The vertical structure functions are the solutions of:

$$(F_{nz}/N^2)_z + c_n^{-2} F_n = 0 \quad (4)$$

with $F_{nz} = 0$ at the surface and at the bottom of the ocean, and where c_n is the phase speed associated to the mode n.

The horizontal equations of motion are:

$$u_{nt} - f.v_n = r.u_n + A_h (u_{nxx} + u_{nyy}) + \tau^x/D_n + p_{nx}/\rho_0 \quad (5)$$

$$v_{nt} - f.u_n = r.v_n + A_h (v_{nxx} + v_{nyy}) + \tau^y/D_n + p_{ny}/\rho_0 \quad (6)$$

$$p_{nt} + \rho_0.c_n^{-2}.(u_{nx} + v_{ny}) = 0 \quad (7)$$

where the horizontal diffusivity coefficient A_h is 10^7 cm^2/s, τ^x and τ^y are the zonal and meridian components of the wind stress forcing, N the Brünt-Väisälä frequency, D_n the wind coefficient relative to each mode, ρ_0 the mean density of sea water over the column and r is a friction coefficient.

No-slip boundary conditions are used on all the boundaries. The time step grows from one to four hours with the mode index n (n = 1 to 3). A further description of this model can be found in Arnault (1984), Arnault *et al.* (1990) and Bourlès (1990). The model is spun up over seventeen years using the Hellerman and Rosenstein (1983) climatological wind stress and then run with 1985-1988 monthly wind stress (Servain *et al.*, 1987).

An important characteristic of our model is its linearity; thus only one asymptotic solution exists at a given time for a given initial condition and a given wind forcing.

Philander *et al.* (1987] have shown that mass field initialization seem to produce better results than velocity field intialization in their general circulation model. However, analytical and numerical studies of data assimilation in tropical oceans (Anderson and Moore, 1986; Moore *et al.*, 1987) show that the best type of data to assimilate depends on the energetic balance (which is essentially dependent on the dissipation) of the model: mass field data are better than velocity field data when potential energy is larger than kinetic energy and *vice versa* when kinetic energy is larger than potential energy. An energetic study of our dissipative model, made from a reference simulation, shows that the total potential energy (sum of energies relative to the three baroclinic modes of the model) exceeds the total kinetic

energy everywhere in the basin (Bourlès *et al.*, 1992). Therefore, we decided to use this linear vertical mode model to assimilate altimetric data in the tropics.

The dynamic height is defined as:

$$H(p_1/p_2) = \int_{p_1}^{p_2} \alpha(S, T, p)\, dp - \int_{p_1}^{p_2} \alpha(35, 0°C, p)\, dp \qquad (8)$$

where α is the specific volume of sea water, defined as being the inverse of *in situ* density. This density is related to pressure by the hydrostatic equation. Thus, from (3) we have:

$$\partial p/\partial z = -\rho'.g = \sum_{n=1}^{3} p_n(x, y, t).dF_n(z)/dz \qquad (9)$$

Using the equation of state of Millero and Poisson (1981) for density, we obtain the dynamic height expression:

$$H(p_1/p_2) = H_{ref} - H_0 + \sum_{n=1}^{3} p_n.Y_n \qquad (10)$$

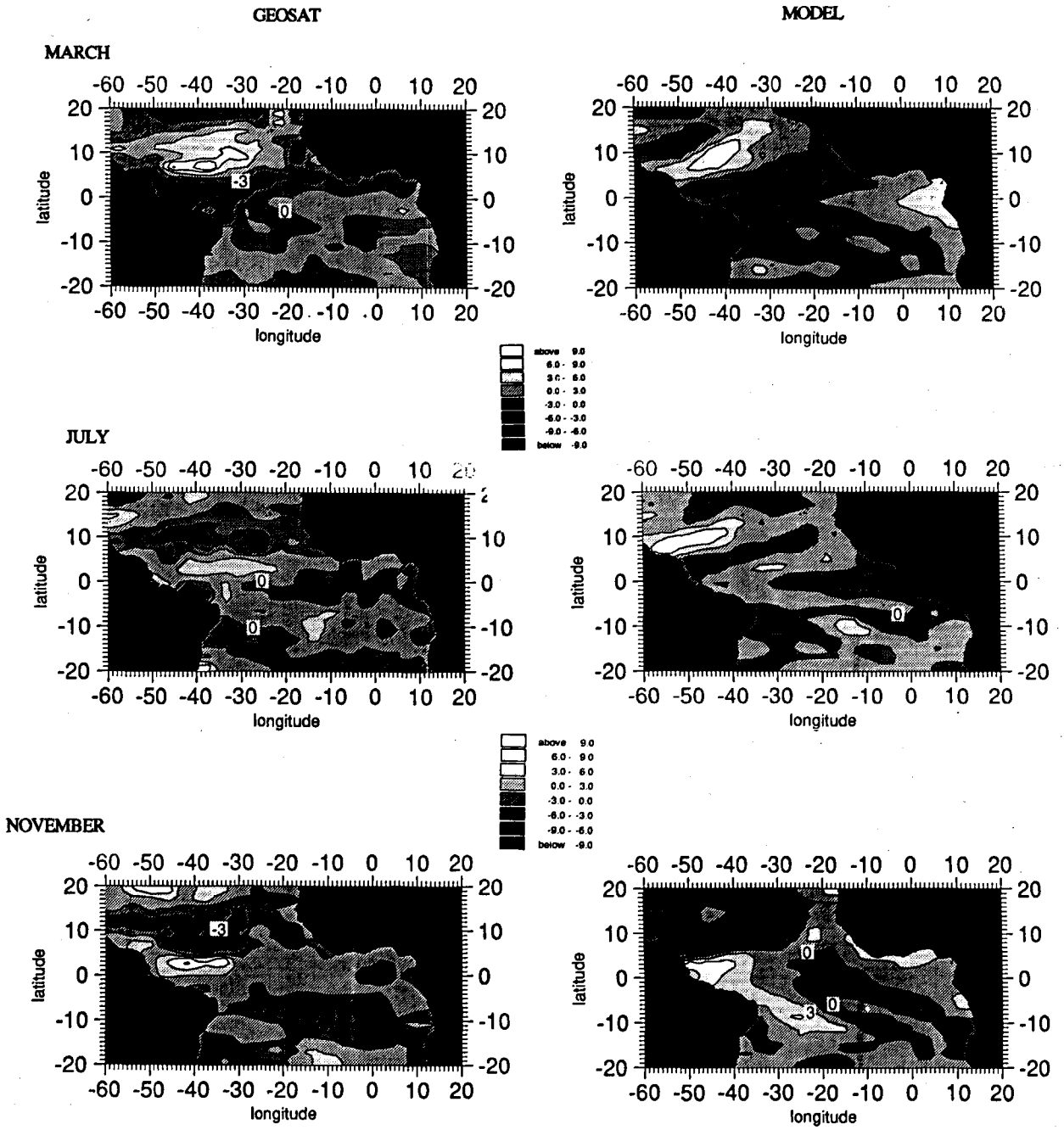

Figure 1

Dynamic height anomaly fields obtained in March (upper panels), July (middle panels) and November 1987 (lower panels) from altimetric data of Geosat (left) and the linear model (right).

Champs d'anomalies de hauteur dynamique : en mars (en haut), juillet (au milieu) et novembre 1987 (en bas), obtenus à partir des données altimétriques de Geosat (à gauche) et du modèle linéaire (à droite).

with

$$H_{ref} = \int_{p_1}^{p_2} (1 - R)/\rho)\, dp;\ H_0 = \int_{p_1}^{p_2} (1/\rho\ (35, 0, p)\, dp$$

and $$Y_n = \int_{p_1}^{p_2} [(1 - R)/g.\rho^2].(dF_n/dz)\, dp$$

where R = p/K, and K is the bulk coefficient.

The altimetric data

Altimetric data are now available for the observing periods of the Geos-3, Seasat and Geosat satellites. They have been shown to be useful for studying the oceanic surface circulation (Cheney *et al.*, 1983; Ménard, 1983]. Successful results have been obtained using altimetric data in tropical regions, despite the difficulty of extracting the large-scale signal due to long wavelength satellite orbit errors, atmospheric errors and oceanic errors. Périgaud *et al.* (1986) have studied the zonal slope of the Indian Ocean from the three months of Seasat data, while Malarde *et al.* (1987) used the same data to study long equatorial waves in the Pacific and Atlantic Oceans. Ménard (1988) obtained the seasonal variability of the dynamic topography from a combination of Geos-3 and Geosat data, and found very good agreement with historical hydrographic data.

The observations used here are monthly mean anomalies of the surface topography, obtained from Geosat data by Arnault *et al.* (1989], who used the objective analysis developed by De Mey and Robinson (1987) and the repetitive tracks technique of Ménard (1983; 1988) to produce altimetric sea-level anomaly fields at three-day intervals, from November 1986 to November 1988. Monthly anomaly fields were computed for this period, on a 4° in longitude by 2° in latitude grid. The reader is referred to Arnault *et al.* (1990) for further details on the altimetric data processing.

The anomaly fields obtained either from altimetric data or from the model, between January 1987 and November 1988, show a rather good agreement with the typical evolution of the structures over all the basin. They show large zonal bands of alternatively negative (upwelling) and positive (downwelling) values, with strong signals in the northern hemisphere. In the boreal summer-autumn season the equatorial upwelling, starting from the African coasts, gives negative values which are maximal from July to September, and the North Equatorial Counter Current (NECC) is well developed. During the winter-spring season, the equatorial upwelling and the positive values characterizing the NECC disappear, and the structures are less clear.

In the NECC and North Equatorial Current (NEC) regions, about 5° and 10°N respectively, the modelled signals are generally in good qualitative and quantitative agreement with the altimetric data, as can be observed in Figure 1, in March, July and November 1987. Although there are some differences in the East Equatorial Region (EER). According to Ménard (1988]) and Arnault *et al.* (1990), the fields obtained from Geosat altimetric data may appear with relatively weak amplitude in the eastern part of the

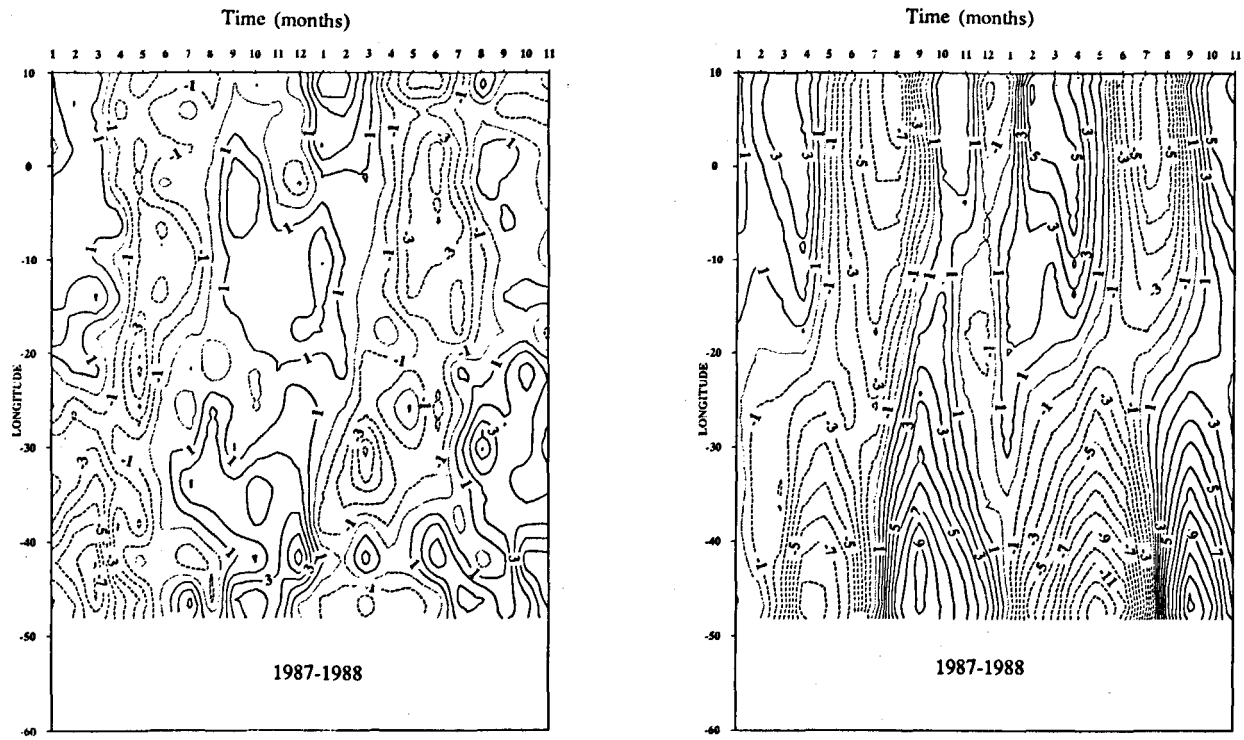

Figure 2

Time evolution during 1987-1988 of dynamic height anomalies from altimetric data of Geosat (left) and the linear model (right) along the equator.

Évolution des anomalies de hauteur dynamique obtenues à partir des données altimétriques de Geosat (à gauche) et du modèle linéaire (à droite) le long de l'équateur en 1987-1988.

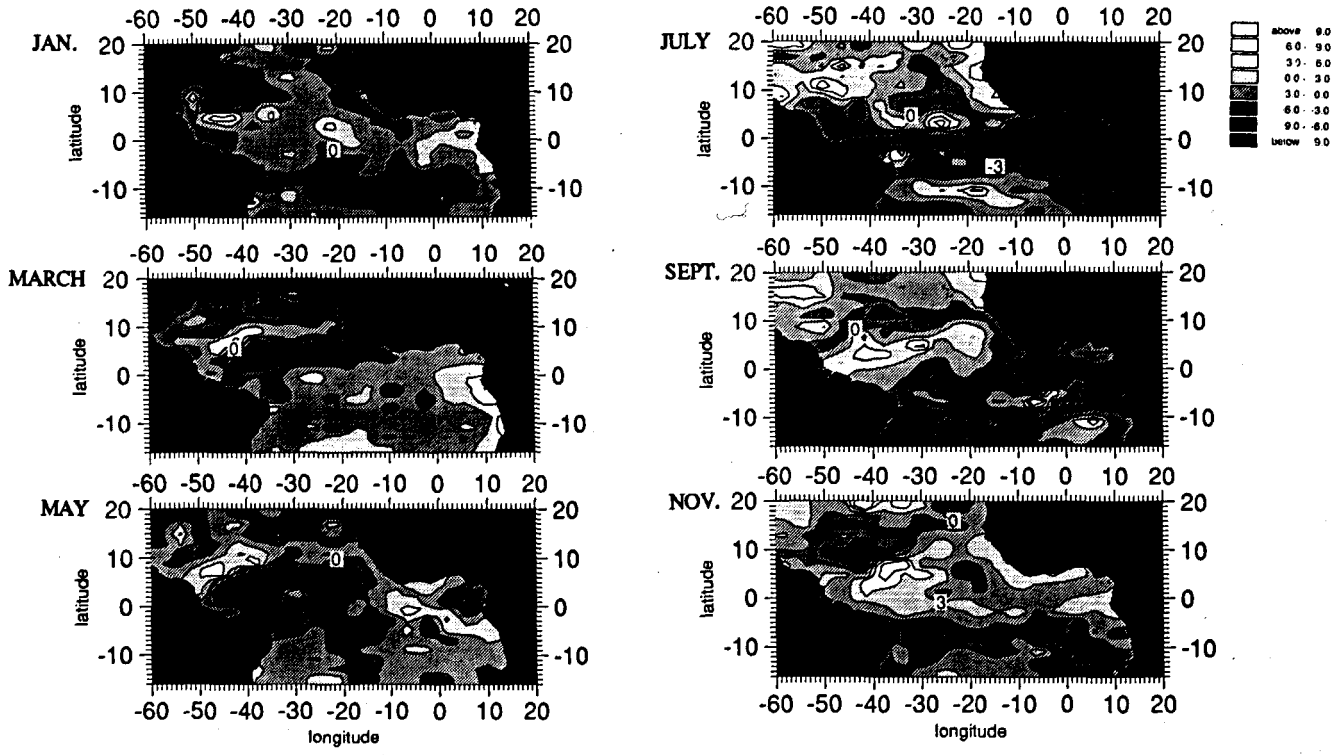

Figure 3

Monthly 0/500 dbar dynamic height anomalies (in dynamic centimetres) for climatological January, March, May, July, September and November, respectively from top to bottom and from left to right.

Champs mensuels des anomalies de hauteur dynamique (en centimètres dynamiques) pour les mois climatologiques de janvier, mars, mai, juillet, septembre et novembre, respectivement de haut en bas et de gauche à droite.

basin, probably because the filtering process of the long wavelength orbit errors may filter a part of the oceanic signal as well. However, Arnault *et al.* (1989) observed a weak equatorial upwelling event in the altimetric data from EER in summer 1987, which has been confirmed by *in situ* observations. It seems that 1987 was affected by a strong inter-annual signal; the upwelling appeared early (in May) in the Gulf of Guinea and had a weak amplitude compared to climatology. The linear model does not capture the anomalies in 1987 (Fig. 1 *b*) due to the absence of the signal in the wind forcing.

The equatorial slope variations obtained from altimetric data have small amplitudes, compared to the modelled ones (Fig. 2). However, the linear model overestimates the equatorial slope, essentially due to the constant density profile chosen in the model, which is not very representative of the EER and West Equatorial Region (WER) where the modelled anomaly values are respectively too low and too high. During 1988, notable differences appear in the WER where the model provides a strong signal, larger than during 1987, contrary to the altimeter data which indicate that the signal is small until September (Fig. 4 to 6 *a* and *b*). On the other hand, both evolutions are closer than during 1987 in the EER and in the Gulf of Guinea, where they show a very pronounced downwelling in winter and spring. However, after the summer equatorial upwelling event, the model produces a strong downwelling from September 1988, stronger than in 1987 and not observed from the altimeter data.

The climatological dynamic height anomaly is shown at two-monthly intervals in Figure 3. This climatology is derived from many years of observations, using a temperature *versus* depth profile through a salinity interpolation, as described by Merle and Arnault (1985). Compared to altimetric data and modelled evolution in 1988 (Fig. 4 to 6 *a* and *b*), and referring to recent studies of Arnault *et al.* (1990) showing an inter-annual event in 1987, 1988 appears quite closer to climatology. Since altimetric data evolution appears clearly close to climatology in the main part of the basin, the model seems to give better patterns in the EER during the summer-autumn season. The lack of variability found for the altimetric signal in this area and at this period of the year, particularly in the Gulf of Guinea, has already been observed by Ménard (1988) and Arnault *et al.* (1990). They suggest that this specific problem is due to the wet tropospheric corrections applied to the raw altimetric data, cloudiness being particularly heavy during summer and autumn in the EER. Further comparisons between altimetry, models and climatology can be found in Arnault *et al.* (1990; 1992).

THE ASSIMILATION TECHNIQUE

Previous studies of data assimilation have dealt with the assimilation of *in situ* observations which correspond to one of the model variables. In this way, the depth of isotherms (or depth of the thermocline) obtained from XBT measure-

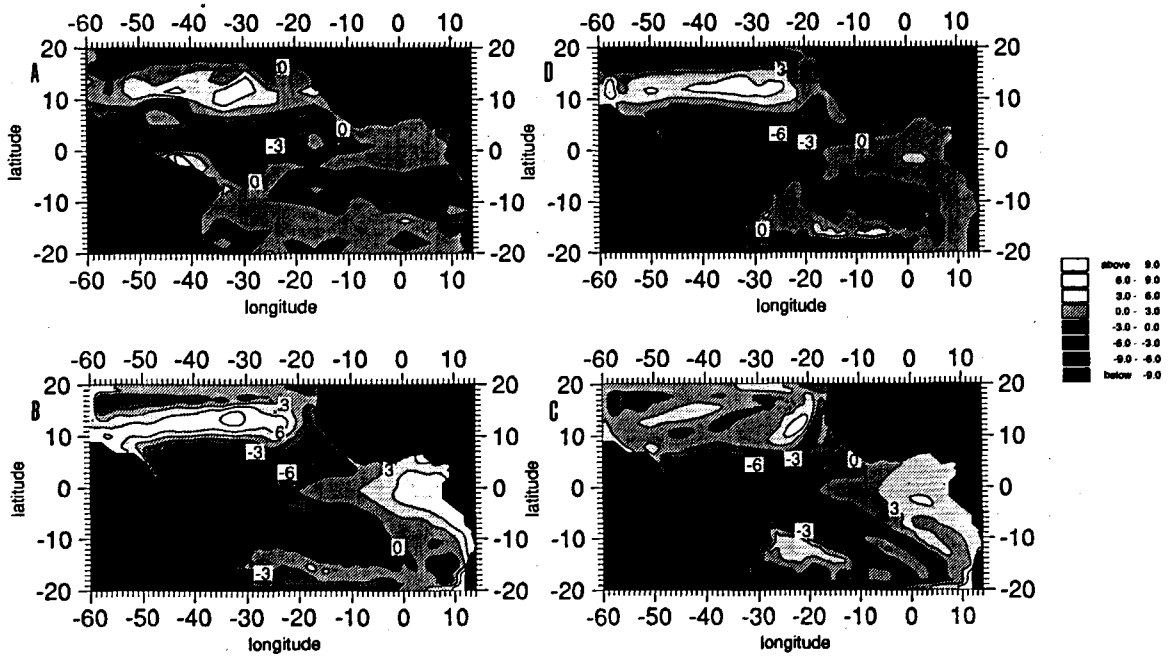

Figure 4

a) Monthly sea level anomalies (in cm) from Geosat altimeter data for March 1988 (top and left); b) monthly 0/500 dbar dynamic height anomalies (in dyn.cm) as computed by the linear model for March 1988 after monthly assimilations in 1987 (bottom and left); c) monthly 0/500dbar dynamic height anomalies (in dyn.cm) as computed by the linear model without assimilation (Control Run) for March 1988 (bottom and right); d) monthly 0/500 dbar dynamic height anomalies (in dyn.cm) as computed by the linear model for March 1988, after monthly assimilations in 1987 and 1988 (top and right).

a) champs mensuels des anomalies de hauteur dynamique (en cm) obtenues à partir des données altimétriques de Geosat en mars 1988 (en haut à gauche) ; b) champs mensuels des anomalies de hauteur dynamique 0/500 dbar (en cm.dyn) simulées par le modèle linéaire en mars 1988, avec des assimilations mensuelles en 1987 (en bas à gauche) ; c) champs mensuels des anomalies de hauteur dynamique 0/500 dbar (en cm.dyn) simulées par le modèle linéaire en mars 1988, sans assimilations (en bas à droite) ; d) champs mensuels des anomalies de hauteur dynamique 0/500 dbar (en cm.dyn) simulées par le modèle linéaire en mars 1988, avec des assimilations mensuelles en 1987 et 1988 (en haut à droite).

ments have been assimilated in a reduced gravity model (Moore *et al.*, 1987; Moore, 1989) and temperature profiles and sea surface temperature in oceanographic general circulation models (Morlière *et al.*, 1989; Leetma and Ji, 1989). Here, we assimilate sea level anomaly fields obtained from altimetry, considered as dynamic height (DH) anomaly fields, which are not direct variables of our model. The difficulty is to project the DH anomaly data on to the first three vertical modes of the model without any loss of information. This means that we have to compute three pressure fields relative to each vertical mode from the DH anomalies, at the time steps when they are available. As shown in the section on "The model", these three pressure fields, which we substitute for those provided by the model, can be easily obtained from the DH through a linear relation.

Thus a method of analysis has been developed. Its formalism is similar to the variational methods of Sasaki (1970) and Provost (1983). The principle is to minimize the difference between the observations and the fields to be estimated, which must be smooth according to defined criteria. The analysis consists in a global minimization of a cost-function over the entire basin. The cost-function J is a linear combination of quadratic terms which correspond to the chosen constraints. An advantage of this method is that many types of constraints (*e. g.* smoothing constraints, dynamic constraints...) can be applied. Furthermore, analyzed fields can be obtained from sparse data at all the grid-points of the model. In this study, the cost-function J used is:

$$J(p_1^*, p_2^*, p_3^*) = \iint [\lambda_d \cdot \sum_{nd=1}^{ND} D^2(p_1^*, p_2^*, p_3^*)/\sigma_{nd}^2] \cdot \delta(x - x_{nd}, y - y_{nd}) + \lambda_l \sum_{n=1}^{3} [L_{x_n}(\partial^2 p_n^*/\partial x^2) + L_{y_n}(\partial^2 p_n^*/\partial y^2)]^2 + \lambda_{gf} \sum_{n=1}^{3} [(p_n - p_n^*)^2/\sigma^2_{p_n})].dx.dy \qquad (11)$$

The first term corresponds to the data constraint and to the projection on the three modes (hereafter the "observation-projection" constraint), the second term is a smoothing constraint, and the third term the first guess-field constraint. In equation (11), ND is the number of observations, p_n is the pressure relative to the -nth mode obtained from the model, p_n^* is the pressure relative to the nth mode obtained from the analysis of the observations, L_x and L_y are the zonal and meridional scales respectively, $\sigma^2_{n_d}$ and $\sigma^2_{p_n}$ are the errors associated with the observations and the first guess-field, λ_d, λ_l and λ_{gf} are normalization and undimentionalization coefficients (*see* further in this section).

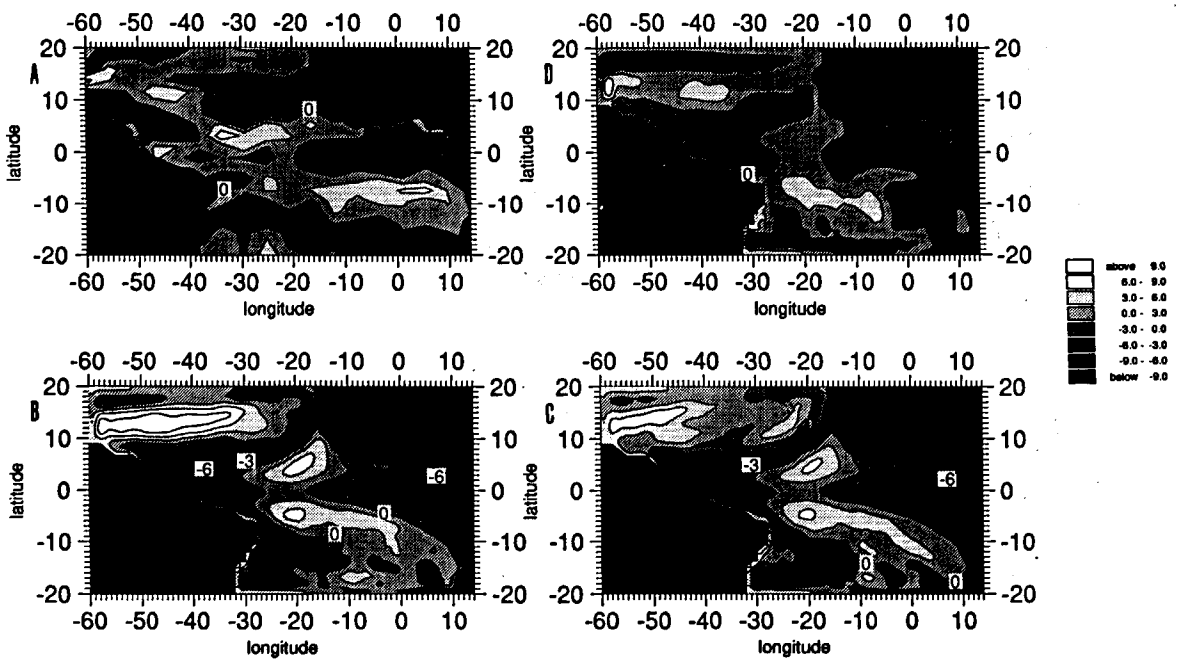

Figure 5

Same as Figure 4, but for July 1988.

Identique à la figure 4, mais pour juillet 1988.

The DH is a function of the pressure fields p_1, p_2 and p_3 (equation 10). The DH anomalies of the model are computed as the difference between the instantaneous DH and the 1987-1988 mean of DH at each grid-point. The "observation-projection" constraint consists of minimizing, at each observation point, the term $(H_{obs}-H^*)$, where H_{obs} is the DH anomaly observation and H^* is a bilinear interpolation to the observation point of the model DH anomalies obtained at the four closest grid-points surrounding the observation point; namely,

$$D(p_1^*, p_2^*, p_3^*) = H_{obs}(x_{obs}, y_{obs}) - H_{ref} + H_0 - \sum_{n=1}^{3} \sum_{i=1}^{4} K_n^i \cdot p_n^*(x_i, y_i) - \bar{H} \quad (12)$$

where $\bar{H}$ is the 1987-1988 mean of the model DH, i is the index of the four grid-points surrounding the observation, n the mode index and K_n^i a coefficient depending on the modes and the interpolation. This constraint takes into account the errors nd associated with the observations. The observational errors σ_{nd}^2 are estimated as equal to the mean of the errors provided by the objective analysis used to obtain the data from Geosat altimeter measurements, after considering measurement errors, filtering process errors, *etc.* (Ménard, 1988). The errors vary from 0.5 cm in the EER and the central regions of the basin to 1.5 cm in the WER.

The anisotropy of the ocean circulation, which is very pronounced in the tropics, appears in the smoothing constraint by considering the zonal and meridional correlation lengths L_x and L_y in the two respective components of the horizontal Laplacian. L_x and L_y are estimated from the fields of the 1987-1988 control run described earlier. These correlation lengths (defined as the zero-crossing of the spatial autocorrelation functions at each grid-point) computed from the model DH fields or the three pressure fields relative to each mode are very similar. Consequently, we shall not consider different L_{xn} or L_{yn} correlation scales for each mode but only use the L_x and L_y scales computed from the model DH fields. L_x decreases from about 2 000 km along the equator to 800 km in high latitudes and L_y increases from about 300 km in the centre of the basin to 1 000 km close to the African and South-American coasts.

The guess-field constraint takes into account the errors σ_{pn}^2 associated with the three pressure fields of the model. As these fields are numerical model results, the determination of the errors is relatively arbitrary. We estimate errors as equal to the time-space variance added to 1/10° of the time variability of each pressure field. Thus, we obtain three estimated error fields constant with time, and errors are more important in the areas with strong variability.

The cost-function J is minimized according to the p_n^*; we obtain a system of NMxNPT linear equations, where NM is the number of modes and NPT the number of grid-points of the model. This system is written in a matrix form, as:

$$J = \lambda_d \mathfrak{D} + \lambda_l \mathfrak{L} + \lambda_{gf} \mathfrak{G} \quad (13)$$

where $\mathfrak{D}$, $\mathfrak{L}$ and $\mathfrak{G}$ are the matrices relative to the "observation-projection", the smoothing and the guess-field constraints respectively. All constraints are considered with the same order of importance; in this way, each coefficient λ_d, λ_l and λ_{gf} is chosen as the inverse of the norm of its respective matrix. Thus, this system is undimensionalized and normalized. It is solved by a conjugate gradient method, which is accelerated by the method of block symmetric over-relaxation (Provost, 1983).

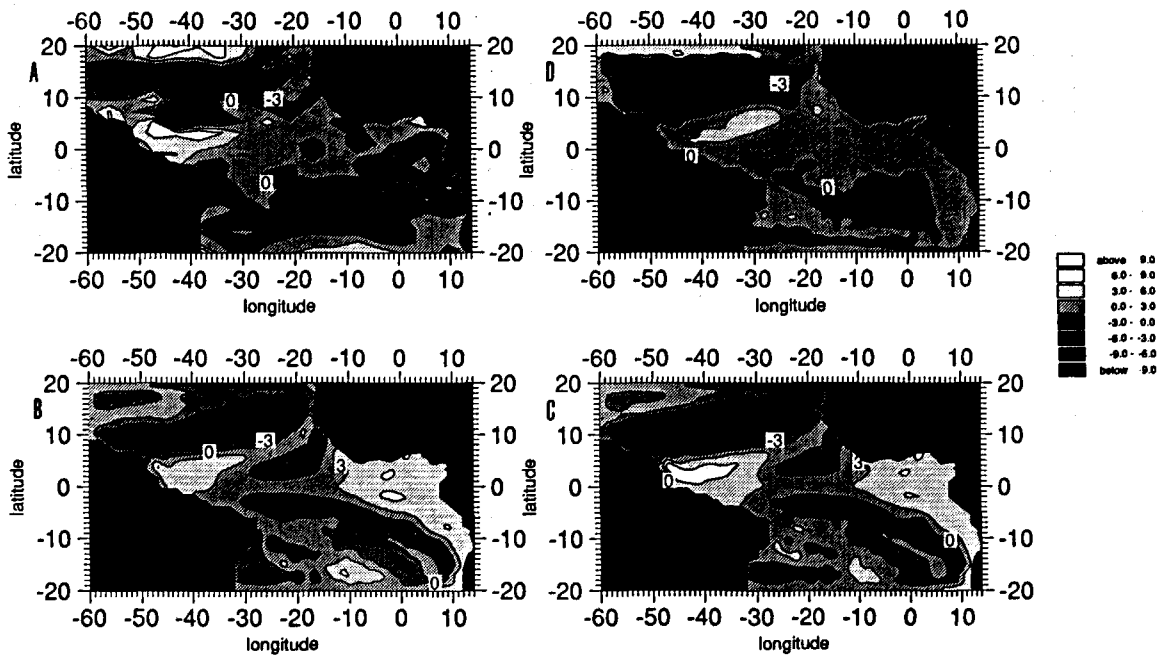

Figure 6

Same as Figure 4, but for November 1988.

Identique à la figure 4, mais pour novembre 1988.

When data are available, the assimilation processing consists in: a) stopping the simulation of the linear model; b) proceeding to the analysis; and c) substituting the fields p_n^* obtained from the analysis for the three pressure fields p_n (the guess field). Then we restart the simulation and the linear model is only driven by the monthly wind stress, until the next update. As the model is linear, the analysis errors may be easily estimated and their computation can be made simultaneously with the analysis. Further details on the method and the analysis errors can be found in Bourlès (1990) and Bourlès *et al.* (1992).

ALTIMETRIC DATA ASSIMILATION

In the first experiment, we assimilate the monthly mean fields of anomalies obtained from Geosat measurements on the 15th day of each month for 1987 after which the model is forced only by the wind during 1988. In a second experiment, data are assimilated on the 15th day of each month for all of 1987 and 1988. The fields described in the following are the fields produced by the model on each 15th day of each month, one month after the last assimilation, and before the variational analysis is performed.

The global and quantitative impact of data assimilation in 1987

As a diagnostic, we compare the evolutions of the root mean square (rms) difference between the altimetric observations (ALT) and the control-run (CR) and of the rms difference between ALT and the fields obtained during the simulation with data assimilation (ASS). Note that the altimetric data values are in centimetres, and DH anomalies are in cm.dyn. The ratio between these two units is the coefficient $\rho_0.g$ that is equal to $1.003.10^{-3}$ c.g.s. So, errors made by mixing these units are negligible compared to observation or model result errors.

During 1987, we observe a very effective improvement of the simulation. The model results are in good agreement with the observations when data assimilation is performed. A comparison of (ALT-CR) and (ALT-ASS) errors is shown in Figure 7, for different regions. The data assimilation procedure improves the fit between the model and the obervations (ALT) by up to 1.5 cm over the entire basin, in the zonal equatorial band and in the EER, and by up to 2 cm in the WER. During August 1987, in the Gulf of Guinea, the improvement reaches 2.7 cm, due to a strong attenuation of the equatorial upwelling simulated by the model, and which is not observed from the altimeter data, as discussed in the section on "The altimetric data". In the WER, improvement reaches 2.7 cm off coasts of Brazil, where the simulated positive anomalies, which characterize the NECC, are closer to the coast and stronger after data assimilation in agreement with altimetric observations (not shown). During 1988, after the last assimilation, we observe a growth of the (ALT-ASS) errors. This phenomenon is due to the linear model relaxing back to its own equilibrium state with the only wind forcing and to the new initial conditions, imposed by the last update. In the low latitudes (WER, EER and zonal equatorial region), the (ALT-ASS) errors increase toward the initial (ALT-CR) errors very rapidly, and both evolutions are similar after five months. Over the whole basin, the new equilibrium state is not reached one year after the last update due to the high

latitudes, where the time adjustement of the waves is slower than in low latitudes. In the EER and the zonal equatorial region, the (ALT-ASS) errors become larger than the initial (ALT-CR) errors, from one to two months after the last update. This is due to perturbations that develop in the EER, already observed in earlier data assimilation experiments in the tropics (Moore, 1989; Bourlès *et al.*, 1992]. When the differences between the observations and the model are relatively large, the assimilation process generates equatorial Kelvin and Rossby waves which propagate along the equatorial wave guide. Kelvin waves are generated in the western part of the equatorial basin. These waves propagate eastward, and generate westward equatorial Rossby waves when reaching the African coast after one month (first baroclinic mode time to cross the basin along the equator), as can be observed in Figure 8. Thus, from January to April-May 1988, the absolute values of the differences are increased by about 1cm in the east, and we also observe in the west during March-April an increase in these differences (Fig. 8), with the same amplitude of 1 cm (which is of the same order than model and observation errors). The wave generation may be explained by the fact that we do not constrain the assimilated pressure fields to satisfy the model dynamics. So, these fields do not agree with the linear response of the model to the wind forcing, and equatorial waves are produced during the readjustment of the model to this single forcing after the data assimilation ceases. Moore (1989) observed the same phenomena by assimilating XBT data in a reduced-gravity model of the tropical Pacific Ocean (Moore and Anderson 1989). He vainly attempted to suppress this complex dynamic problem, causing greater damage on the simulations in the eastern part of the basin. We did not study means of alleviating this problem by adding other constraints in our analysis, but we have shown that these wave propagations are stopped by successive reinitializations (Bourlès, 1990; Bourlès *et al.*, 1992). It seems that only complex assimilation techniques, such as the adjoint technique or Kalman filter, may make it possible to avoid this kind of problem by taking into account previous knowledge about model and data errors; but these techniques are still very costly in computing time. Using an adjoint method, Sheinbaum and Anderson (1990) did not generate spurious waves in assimilating XBTs data in a linear gravity model.

However, we see a strong improvement of the differences during 1987, reaching 4 cm in the WER and 3 cm in the EER during summer, due to the attenuation of the modelled upwelling (Fig. 7). The positive (ALT-CR) differences

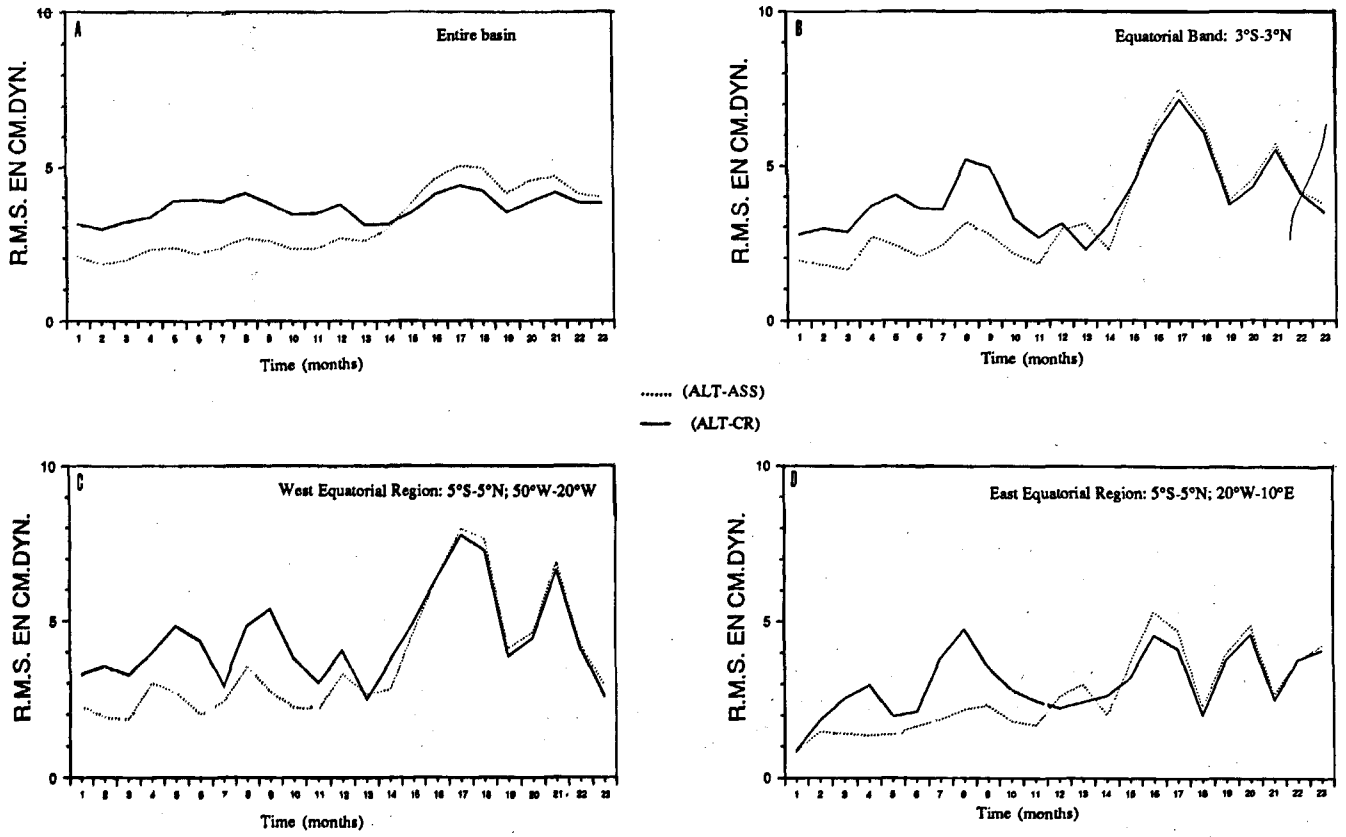

Figure 7

Time-series of the root mean square (rms) differences between the control run (CR) and the altimetric observations (ALT) (full line) and between ALT and the fields obtained during the simulation with data assimilations in 1987 (ASS) (dashed line), computed during 1987-1988: a) over the entire basin; b) in the equatorial band limited to 3°S-3°N; c) in the western equatorial region limited to 5°S-5°N in latitude and to 20°W-50°W in longitude; and d) in the eastern equatorial region limited to 5°S-5°N in latitude and to 20°W-10°E in longitude.

Évolution, en 1987 et 1988, des différences quadratiques moyennes entre la simulation de contrôle (CR) et les observations altimétriques (ALT) (traits pleins) et entre ALT et les champs obtenus pendant la simulation avec assimilations en 1987 (ASS) (en pointillés), calculées : a) sur tout le bassin ; b) dans la bande équatoriale limitée aux latitudes 3°S-3°N ; c) dans la région ouest-équatoriale limitée aux latitudes 5°S-5°N et aux longitudes 20°W-50°W ; et d) dans la région est-équatoriale limitée aux latitudes 5°S-5°N et aux longitudes 20°W-10°E.

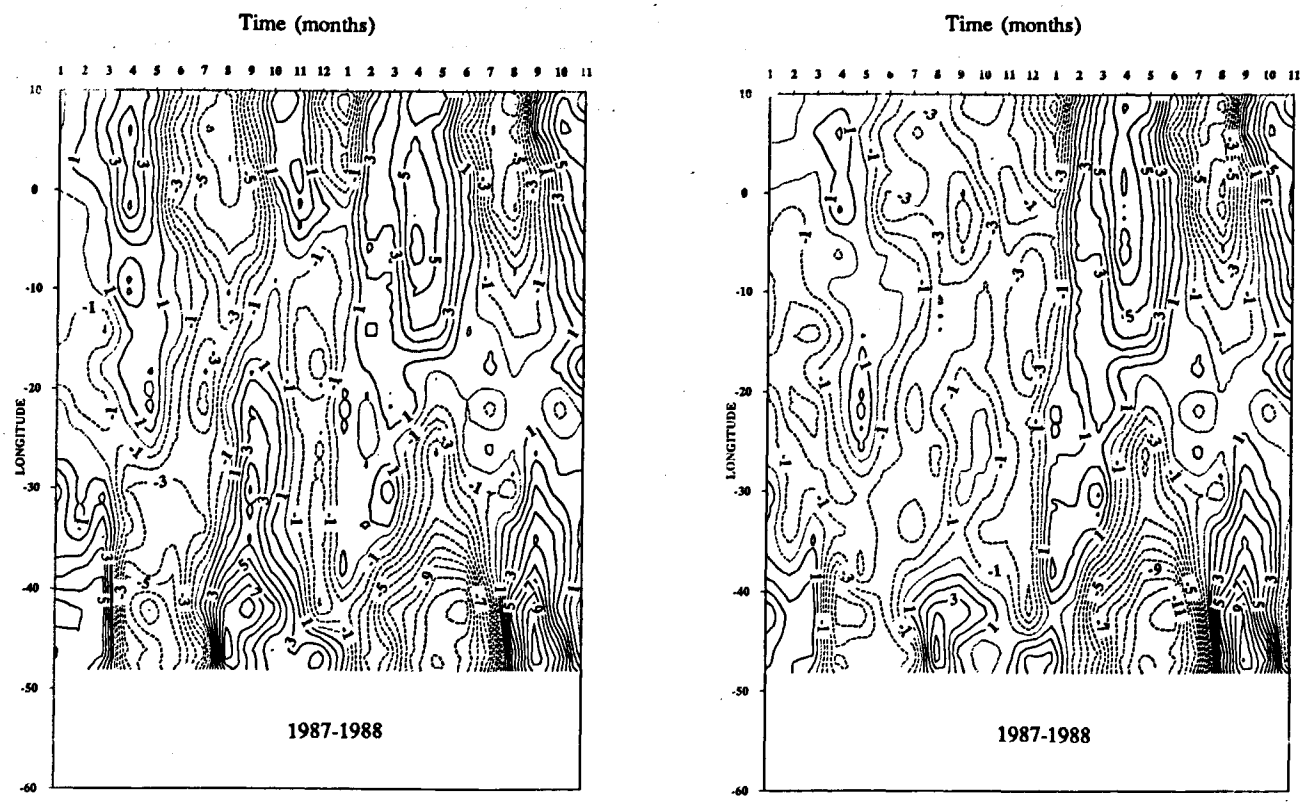

Figure 8

Evolution during 1987-1988 of dynamic height anomaly differences along the equator: left) between the control run (CR) and the altimetric observations (ALT); right) between ALT and the fields obtained during the simulation with assimilations in 1987 (ASS).

Évolution en 1987-1988 des différences d'anomalies de hauteur dynamique le long de l'équateur : à gauche) entre la simulation de contrôle (CR) et les observations altimétriques (ALT) ; à droite) entre ALT et les champs obtenus pendant la simulation avec assimilations en 1987 (ASS).

along the West African coast in October and November 1987, when the model was providing a downwelling not observed by the Geosat altimeter, have disappeared (not shown) and the simulated equatorial slope is consequently reduced as a result of data assimilation (Fig. 8).

Qualitative impact of assimilations in 1987 and 1988

Figures 4 to 6 show the fields obtained in March, July and November 1988, after data was assimilated only during 1987 (Fig. 4 *b*, 5 *b* and 6 *b*) and after data was assimilated during 1987 and 1988 (Fig. 4 *d*, 5 *d* and 6 *d*). Comparing the simulations after data assimilation only during 1987 with the observations (Fig. 4 *a*, 5 *a* and 6 *a*), we note that the "forecast", even if forecasting is not very representative by using a linear model, is strongly improved during the first three months, outside the equatorial band limited to the 3°S and 3°N latitudes (Fig. 4). This is essentially true in the northern hemisphere, and in the NECC region, where the signals are large. Later in the year, we can observe between 10° and 15°N an irrealistic growth of the intensity of the NEC, due to the slower return to the model equilibrium (the geostrophic adjustment is longer and the phase velocity of the waves increases with latitude) and influences of the closed boundaries (Fig. 5).

The simulation with assimilations during 1988 (Fig. 4 *d*, 5 *d* and 6 *d*) indicates that the monthly reinitializations of the model:

a) effectively improve the simulation in the EER. From February to May 1988, the strong downwelling simulated in the Gulf of Guinea, and not observed with altimeter data, is suppressed. The summer-autumn upwelling is attenuated down to 3 cm, in agreement with the observations. In the same way, the upwelling modelled in November is totally suppressed.

b) consequently reduce the overestimation of the equatorial slope simulated by the linear model (6 cm instead of 12 cm in March, in agreement with the slope obtained from altimeter data).

c) in higher latitudes, reduce the simulated amplitude of the NECC in summer-autumn season, in agreement with altimetric observations, and suppress the simulated signals in the southern hemisphere not observed by the Geosat altimeter.

On the other hand, the strong anomalies located along the coasts of Brazil and Guyana, observed from Geosat measurements, are not reproduced by the assimilation run. These structures are strongly suppressed by the analysis, because of the larger length scales used in the smoothing constraint (*see* above). Likewise, we see that short scale structures appear north of 15°N and south of 15°S. That is explained by an energy accumulation along the boundaries, coming from waves propagating poleward along the African coast and reflected along the closed frontiers.

SUMMARY AND CONCLUSION

In this study, we have used a simple linear model of the tropical Atlantic, providing a representative simulation of the DH variability, and we have developed an assimilation technique to test altimetric data assimilation experiments. The assimilation of DH anomaly fields obtained from the Geosat altimeter, though of weak amplitudes, were found to improve the model simulations effectively. As representative fields of dynamic topography can today be obtained from altimetric measurements (Ménard, 1988; Arnault *et al.*, 1989), we have shown that we can successfully assimilate altimetric data in a model with an adapted analysis method, in the same manner as *in situ* data.

However, the observation errors and the model errors are difficult to quantify precisely, and are of the same order as the signal in any areas of the basin. Consequently, the quality of the improvements obtained with this method can only be confirmed in the areas of large variability, such as WER and EER, and the NECC region in summer-autumn. In order to obtain statistically representative results, the accuracy of the altimetric measurements must be improved (this will be achieved with ERS1 and the Topex-Poseidon satellite), as well as the estimation and the reduction of the model errors. Techniques taking into account the dynamics of the models and computing the time evolution of the error covariance have to be used to apply altimetric data assimilations, which are likely to improve complex model simulations, their validation and the parameterizations of short-scale processes themselves.

Aknowledgements

The authors wish to thank J. Merle of ORSTOM/Paris for encouragement and support, and Y.Ménard and P. Vincent (CNES/Toulouse) for interesting comments and altimetric data processing. We also wish to express our gratitude to the team of the CCR (Centre de Calcul Recherche) of the University Paris-VI for constant and precious assistance. B.Bourlès and S.Arnault were supported by ORSTOM and C. Provost by CNRS.

REFERENCES

Anderson D.L.T. and A.M. Moore (1986). Data assimilation. *Adv. phys. ocean. Num. Model.*, J.J. O'Brien, editor. D. Reidel Publishing Company, 437-464.

Arnault S. (1984). Variations saisonnières de la topographie dynamique et de la circulation superficielle de l'Océan Atlantique tropical. *Thèse, Université Pierre et Marie Curie, Paris VI, France*, 186 pp.

Arnault S., Y. Ménard and M.-C. Rouquet (1989). Variability of the tropical Atlantic in 1986-1987 as observed by Geosat and *in situ* data. *Adv. Space Res.*, **9**, 7, 383-386.

Arnault S., Y. Ménard and J. Merle (1990). Observing the tropical Atlantic Ocean in 1986-1987 from altimetry. *J. geophys. Res.*, **95**, C10, 17, 921-945.

Arnault S., A. Morlière, J. Merle and Y. Ménard (1992). Low-frequency variability of the tropical Atlantic surface topography: altimetry and models comparison, to be published in *J. geophys. Res.*

Bourlès B. (1990). Assimilation de données de hauteur dynamique dans un modèle linéaire appliqué à l'Océan Atlantique tropical. *Thèse de Doctorat, Université Pierre .et Marie.Curie, Paris VI, France.*

Bourlès B., S. Arnault and C. Provost (1992). Towards altimetric data assimilation in a tropical Atlantic model, to be published in *J. geophys. Res.*

Cheney R.E., J.G. Marsh and B.D. Beckley (1983). Global mesoscale variability from colinear tracks of Seasat altimeter data. *J. geophys. Res.*, **88**, 4343-4354.

Delcroix T and C. Gautier (1987). Estimates of heat content variations from sea level measurements in the central and western tropical Pacific from 1979 to 1985. *J. phys. Oceanogr.*, **17**, 6, 725-734.

De Mey P., and A. Robinson (1987). Assimilation of altimeter eddy fields in a limited area quasi-geostrophic model. *J. phys. Oceanogr*, **17**, 2280-2293.

du Penhoat Y., and A.-M. Tréguier (1985). The seasonal linear response of the tropical Atlantic Ocean. *J. phys. Oceanogr.*, **15**, 316-329.

du Penhoat Y., and Y. Gouriou (1987). Hindcasts of equatorial sea surface dynamic height in the Atlantic in 1982-1984. *J. geophys. Res.*, **92**, C4, 3729-3740.

Hellerman S. and M. Rosenstein (1983). Normal monthly wind stress over the world ocean with error estimates. *J. phys. Oceanogr.*, **13**, 1093-1104.

Leetma A. and M. Ji (1989). Operational hindcasting of the tropical Pacific. *Dyn. atmos. Oceans*, **13**, 465-490.

Malarde J.-P., P. De Mey, C. Périgaud and J.-F. Minster (1987). Observation of long equatorial waves in the Pacific Ocean by Seasat altimetry. *J. phys. Oceanogr.*, **17**, 2273-2279.

Ménard Y. (1983). Observation of eddy fields in the Northwest Atlantic and Northwest Pacific by Seasat altimeter data. *J. geophys. Res.*, **88**, 1853-1866.

Ménard Y. (1988). Observing the seasonal variability in the tropical Atlantic from altimetry. *J. geophys. Res.*, **93**, C11, 13, 967-13,978.

Merle J. and S. Arnault (1985), Seasonal variability in the equatorial Atlantic Ocean. *J. mar. Res.*, **43**, 267-288.

Miller L. and R.E. Cheney (1990). Large-scale meridional transport in the tropical Pacific Ocean during the 1986-1987 El Niño from Geosat. *J. geophys. Res.*, **95**, C10, 17, 905-921.

Miller L., R.E. Cheney and D. Milbert (1986). Sea-level time series in the equatorial Pacific from satellite altimetry. *Geophys. Res. Letts*, **13**, 375-478.

Millero F. and A. Poisson (1981). International one atmosphere equation of state of seawater. *Deep-Sea Res.*, **28A**, 6, 525-529.

Moore A.M. (1989), Aspect of geostrophic adjustement during tropical ocean data assimilation. *J. phys. Oceanogr.*, **19**, 435-461.

Moore A.M. and D.L.T. Anderson (1989). The assimilation of XBT data into a layer model of the tropical Pacific Ocean. *Dyn. atmos. Oceans*, **13**, 441-464.

Moore A.M., N.S. Cooper and D.L.T. Anderson (1987). Initialization and data assimilation in models of the Indian Ocean. *J. phys. Oceanogr.*, **17**, 1965-1977.

Morlière A., G. Reverdin and J. Merle (1989). Assimilation of temperature profiles in a oceanic general circulation model for a continuous survey of tropical Atlantic. *J. phys. Oceanogr.*, **19**, 12, 1892-1899.

Périgaud C., J.-F. Minster and G. Reverdin (1986). Zonal slope variability of the tropical Indian Ocean studied from Seasat altimetry. *Mar. Geod.*, **10**, 53-67.

Philander R.G.H. and R.C. Pacanowski (1984). Pictures from a simulation of the seasonal cycle of the tropical Atlantic Ocean. Publication NOAA.

Philander R.G.H. and R.C. Pacanowski (1986). A model of a seasonal cycle in the tropical Atlantic. *J. geophys. Res.*, **91**, C12, 14192-14206.

Philander R.G.H., S.G.H. Hurlin and R.C. Pacanowski (1987). Initial conditions for a general model of tropical oceans. *J. phys. Oceanogr.*, **17**, 147-157

Provost C. (1983). A variational method for estimating the general circulation in the ocean. *Ph. D. thesis, University of California, San Diego, California, USA.*

Sasaki Y. (1970). Some basic formalisms in numerical variational analysis. *Mon. Weath. Rev.*, **98**, 875-883.

Servain J., M. Serva, S. Lukas and G. Rougier (1987). Climatic atlas of the tropical Atlantic wind stress and sea-surface temperature 1980-1984. *Ocean-air Interactions*, **1**, 109-182.

Sheinbaum J. and D.L.T. Anderson (1990). Variational assimilation of XBT data. Part 2: Sensivity studies and use of smoothing constraints. *J. phys. Oceanogr.*, **20**, 689-704.